Supporting Information for

Virtual ultrasound machine operating in a GHz to MHz frequency range for particle-based biomedical simulations

Urban Čoko, Tilen Potisk and Matej Praprotnik

Matej Praprotnik
E-mail: praprot@cmm.ki.si

This PDF file includes:

Supporting text
Figs. S1 to S7
Tables S1 to S5
SI References

Supporting Information Text

A. Scaling of dimensionless quantities. To ensure numerical stability and ease of use, all simulations in this study are expressed in dimensionless form. The user defines three fundamental reference scales—length, time, and density—from which all other physical quantities, such as mass, energy, and viscosity, are derived. The dimensionless temperature is expressed in terms of thermal energy as $T^* = k_B T/E_0$, where k_B is the Boltzmann constant, E_0 is the energy scale, and the superscript asterisk denotes a dimensionless quantity. A change in simulation scale (granularity) is implemented by multiplying both the characteristic length and time by a constant factor. Since the timestep is constrained by the time required for an acoustic signal to traverse one cutoff distance, the cutoff and the maximum stable timestep increase proportionally under such scaling. This procedure maintains a constant non-dimensional speed of sound. Typical scales, used in the article are given in Table S1. Most terms in the non-dimensional equation of motion (1) are invariant under this scaling transformation. The only quantities that vary are the dimensionless viscosity and temperature, which adjust according to the following relations when the simulation scale is increased by a factor of ten:

$$\eta^*_{\text{before}} = \frac{\eta}{\eta_0} \to \frac{\eta}{10\eta_0} = \eta^*_{\text{after}} = \frac{1}{10}\eta^*_{\text{before}}$$
$$T^*_{\text{before}} = \frac{k_B T}{E_0} \to \frac{k_B T}{10^3 E_0} = T^*_{\text{after}} = \frac{1}{1000}T^*_{\text{before}}.$$

In these expressions, the subscripts "before" and "after" indicate values prior to and following the scaling transformation, respectively, while the subscript "0" denotes the base scale derived from the three fundamental reference scales.

Table S1. Simulation Scales (Granularities)

Length Scale	Time Scale
$1 \times 10^{-8}\,\text{m}$	$1 \times 10^{-9}\,\text{s}$
$1 \times 10^{-7}\,\text{m}$	$1 \times 10^{-8}\,\text{s}$
$1 \times 10^{-6}\,\text{m}$	$1 \times 10^{-7}\,\text{s}$

B. Analysis of the fluid in equilibrium. In this section, we compare the novel usSDPD method with the standard (vanilla) SDPD implementation. To evaluate the stability of the investigated methods, we simulate a fluid in equilibrium and monitor the density of a representative particle over time, as shown in Figure S1. Simulation parameters are listed in detail in the Supplementary Information, Section C. Figure S1b reveals that, at a time scale of $2 \times 10^{-9}\,\text{s}$, vanilla SDPD method exhibits non-physical pressure fluctuations. These oscillations disappear only when the time scale is reduced to $1 \times 10^{-9}\,\text{s}$, as shown in Figure S1a. In contrast, usSDPD shows an approximately 40 times larger stable timestep length (Figures S1c and S1d).

Figure S2 shows that the mean-square displacement (MSD) curves exhibit linear behavior both for vanilla SDPD and usSDPD methods, indicating the absence of freezing artifacts at the studied scales. In contrast, ordinary DPD displays a horizontal MSD curve, signifying particle freezing. The diffusion coefficients derived here represent the effective diffusion of SDPD particles and do not directly correspond to physical diffusion constants. Nevertheless, as a first approximation, they can be interpreted using the Einstein relation for spherical particles in a low–Reynolds-number fluid,

$$D = \frac{k_B T}{6\pi\eta r}, \qquad [1]$$

where r denotes the particle radius. Using $T = 300\,\text{K}$, $r = 2.5 \times 10^{-8}\,\text{m}$, and $\eta = 8.9 \times 10^{-4}\,\text{Pa s}$ yields $D \approx 1 \times 10^{-11}\,\text{m}^2/\text{s}$, differing by less than an order of magnitude among the two methods. For the usSDPD case, where $r = 1.5 \times 10^{-8}\,\text{m}$, slightly higher diffusion coefficient is obtained, consistent with the results shown in Figure S2b.

The radial distribution functions (RDFs) for the vanilla SDPD and usSDPD are shown in Figure S3. In Figure S3a, the highest RDF peak is located at $r = 0.5 \times 10^{-7}\,\text{m}$, while in Figure S3b the peak shifts to $r = 0.3 \times 10^{-7}\,\text{m}$. These distances correspond to the diameters of the fluid particles used in each model.

To compare the stability of the vanilla SDPD and usSDPD methods at nanoscopic scales, we perform simulations at 10 nm and 1 nm granularities. These regimes are particularly relevant for studying the interaction of terahertz (THz) excitations with biological and soft-matter systems, including proteins, lipid membranes, and other nanoscale structures. As the length scale decreases, the amplitude of thermal fluctuations grows, requiring a reduction in the simulation timestep to maintain numerical stability. Table S2 summarizes the maximum stable time scales for vanilla SDPD and usSDPD methods. At the 1 nm scale, the stability of the two methods rapidly deteriorates. Notably, while the methods maintain stability if timestep is sufficiently reduced, they offer no clear advantage over simpler alternatives, such as DPD. Given these observations, and in light of recent findings by Papež *et al.* (1), we conclude that SDPD-based methods are not well-suited for US simulations at nanometer scales. Instead, the standard DPD method provides a more efficient and robust alternative, and should be preferred in virtual US machine implementations operating at such resolutions.

To evaluate the accuracy of the measured viscosity relative to the input viscosity, we conduct a Couette flow simulation using the OBMD framework. Shear forces are applied within the buffer regions, and the resulting velocity profile is measured

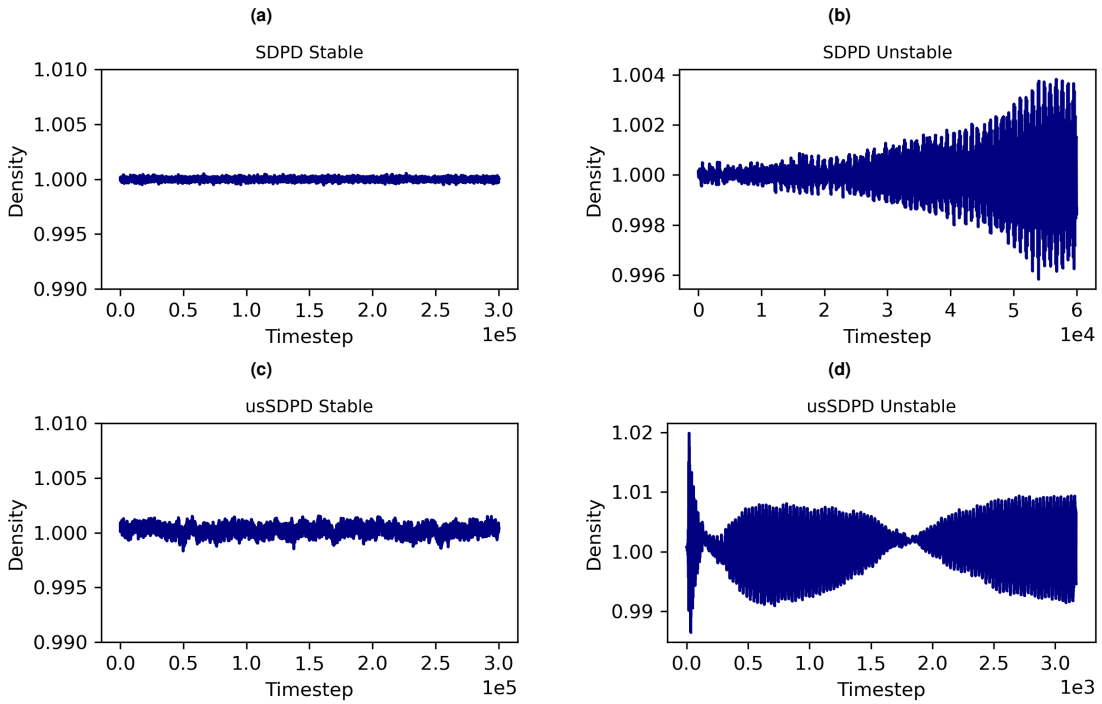

Fig. S1. Stability analysis for SDPD and usSDPD methods on a $0.1\,\mu\mathrm{m}$ granularity. (a) SDPD, time-scale $1 \times 10^{-9}\,\mathrm{s}$, (b) SDPD, time-scale $2 \times 10^{-9}\,\mathrm{s}$, (c) usSDPD, time-scale $4 \times 10^{-8}\,\mathrm{s}$, (d) usSDPD, time-scale $5 \times 10^{-8}\,\mathrm{s}$. The data is left in dimensionless units for clarity.

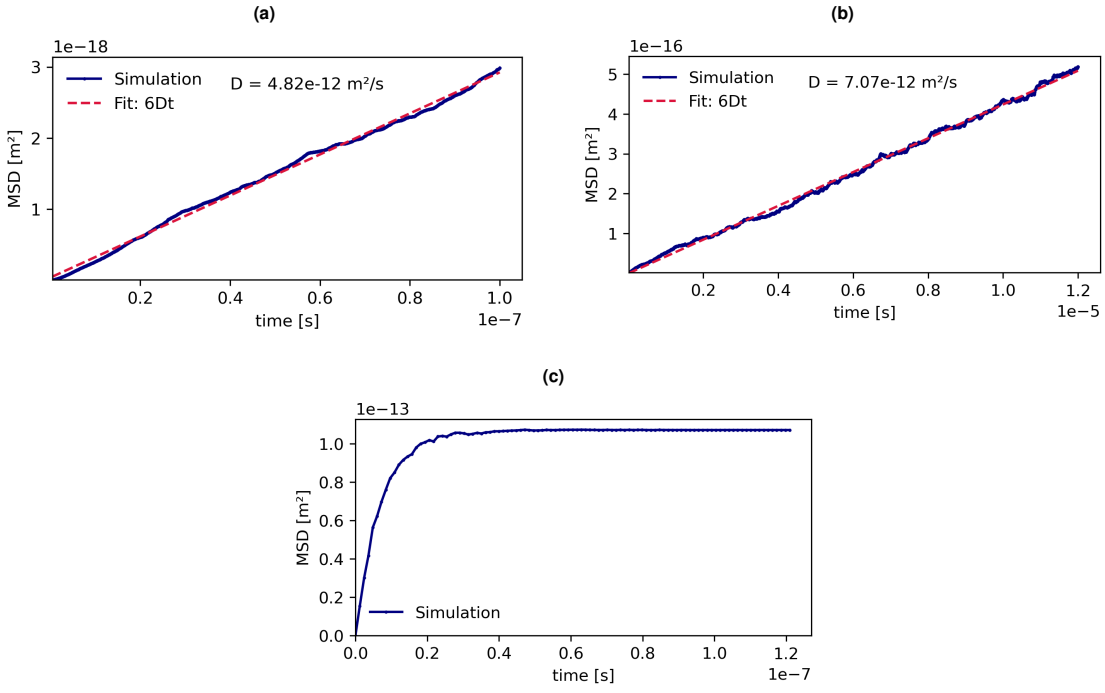

Fig. S2. MSD curves for (a) vanilla SDPD, (b) usSDPD and (c) DPD. Both SDPD and usSDPD simulations are performed at $0.1\,\mu\mathrm{m}$ granularity, the former at time-scale $1 \times 10^{-9}\,\mathrm{s}$ and the latter at $4 \times 10^{-8}\,\mathrm{s}$. The viscosity and the speed of sound are matched to those of water and the temperature is $300\,\mathrm{K}$ in both cases. In the DPD simulation, the scales are chosen, such that the mapping number is $N_m = 10^6$, density is matched to the density of water and the temperature is $300\,\mathrm{K}$. The DPD parameter $a = 10^7$ is obtained by matching the water speed of sound at the desired mapping number and γ is set to 50. While both SDPD and usSDPD show a linear MSD, plain DPD freezes.

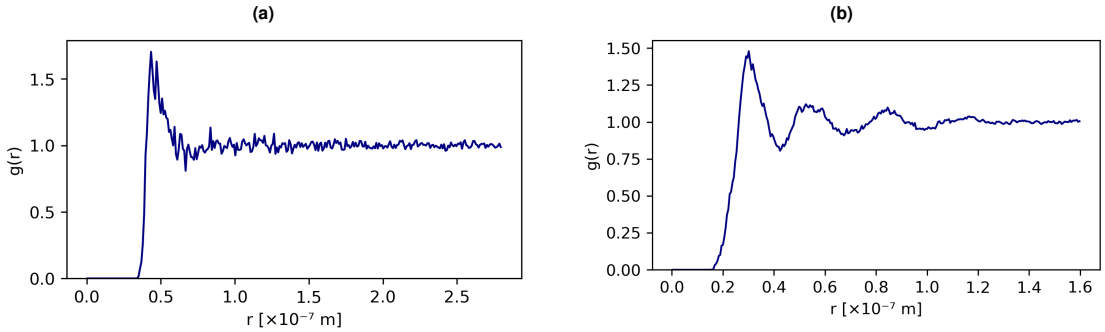

Fig. S3. RDF curves for (a) vanilla SDPD and (b) usSDPD.

(a)

Method	Max Time Scale	Comment
vanilla SDPD	0.5 ns	At timestep 1 ns, simulation crashes after some time.
usSDPD	1 ns	

(b)

Method	Max Time Scale	Comment
vanilla SDPD	0.001 ns	At timestep 0.01 ns, fluid freezes after some time.
usSDPD	0.01 ns	

Table S2. Maximum stable time scale for the vanilla SDPD and usSDPD at nanoscopic length scales. (a) 10 nm length scale, (b) 1 nm length scale. The speed of sound and viscosity match to those of water: $c = 1481\,\mathrm{m/s}$ **and** $\eta = 8.9 \times 10^{-4}\,\mathrm{Pa\,s}$**.**

in the region of interest (see Figure S4). Simulation parameters are listed in detail in the Supplementary Information, Section C. Figure S5a presents the velocity profile for the usSDPD method. As expected, the profile exhibits linear behavior, consistent with theoretical predictions. The simulated viscosity can be extracted from the slope of the profile and is annotated in the figure. We note that the simulated viscosity is slightly higher than the input viscosity, likely due to additional LJ interaction potential. For a slightly reduced input viscosity of $6 \times 10^{-4}\,\mathrm{Pa\,s}$, the measured viscosity is $7.1 \times 10^{-4}\,\mathrm{Pa\,s}$ (see Figure S5b), which demonstrates that, through careful tuning of the input viscosity, it is possible to achieve a simulated viscosity that closely approximates the actual viscosity of water.

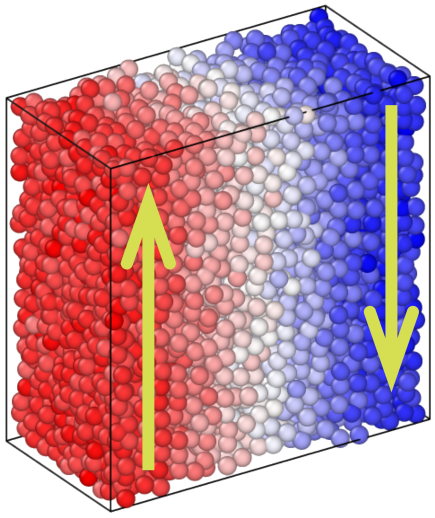

Fig. S4. Snapshot of the Couette flow simulation. Particles are color-coded based on the vertical component of velocity (denoted with arrows).

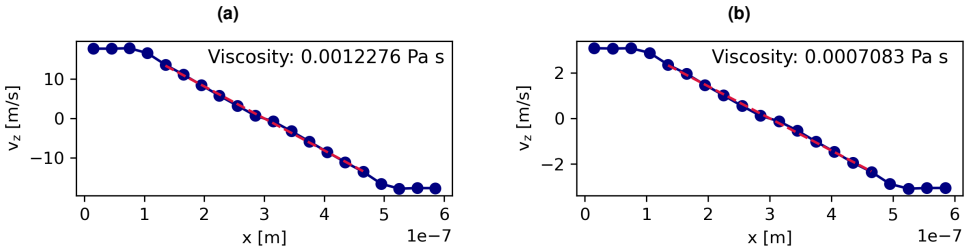

Fig. S5. Velocity profiles for usSDPD. Simulated viscosities are obtained from the slopes of the velocity profiles for input viscosities: (a) 8.9×10^{-4} Pa s and (b) 6×10^{-4} Pa s.

Figure S6 illustrates the establishment of the linear velocity profile in the Couette flow experiment. The profile forms after approximately 1×10^{-7} s, consistent with the analytical estimate of the characteristic start-up time $\tau = \rho h^2/\eta$, where h is the gap between the plates (corresponding to the simulation box width). For a width of 0.6 µm and shear buffer thickness of 0.075 µm, we obtain $\tau \approx 1.7 \times 10^{-7}$ s, which is in agreement with the simulation results.

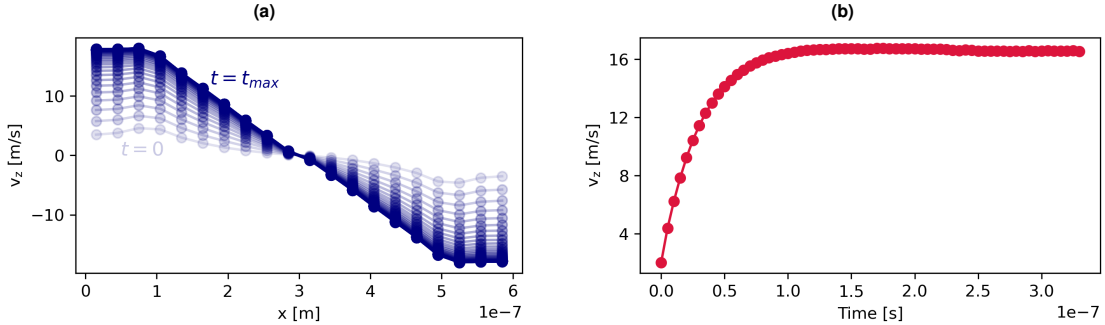

Fig. S6. Viscosity equilibration for usSDPD. (a) Evolution of velocity profile. (b) Temporal evolution of velocity at a fixed position x.

At the 1 µm granularity, the measured viscosity of the usSDPD fluid agrees well with the values obtained at the 0.1 µm granularity, however, the reduced thermal fluctuations lead to the formation of layered structures within the Couette flow (Figure S7), a phenomenon not observed at smaller scales where fluctuations promote particle mixing along the shear velocity gradient. The theoretically predicted equilibration time at this scale is more than five times longer than the value obtained in simulation. Consequently, simulations at the 0.1 µm granularity are employed throughout this study, as they most faithfully reproduce the physical properties of water.

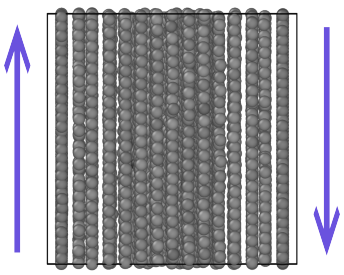

Fig. S7. Snapshot of equilibrium Couette flow at 1 µm granularity. Arrows denote the direction of the applied shear force.

C. Parameters. This subsection summarizes the parameters used in the simulations presented in this paper. Tables S3 and S4 list the parameters employed in the stability and viscosity analyses described in Section 1.1, respectively. The parameters used in the acoustophoresis simulations are given in Table S5.

References

1. P Papež, F Merzel, M Praprotnik, Sub-THz acoustic excitation of protein motion. *J. Chem. Phys.* **159**, 135101 (2023).

Table S3. Common simulation parameters for stability analysis simulations. Parameters beginning with a capital case letter are given in SI units, parameters beginning with a lower case letter are given in dimensionless units. Values in black color are common to both methods, values in green are specific to SDPD and values in blue are specific to usSDPD. Some of the technical parameters are skipped for brevity.

Parameter	Value	Short description
Length scale		
`Length_scale`	1.0×10^{-7}	kernel function cutoff h [m]
Outer fluid parameters		
`Fluid_density`	998.0	density of water [kg/m^3]
`Viscosity`	8.9×10^{-4}	dynamic viscosity of water [Pa s]
`Speed_of_sound`	1481.0	speed of sound [m/s]
`Temperature`	300.0	temperature [K]
`Kb`	$1.3806504 \times 10^{-23}$	Boltzmann constant [J/K]
Simulation parameters		
`skin`	0.2 or 0.12	skin thickness
`particle_diameter`	0.5 or 0.3	particle diameter
`timestep`	0.001	timestep size relative to the time scale
`max_rho_relative_error`	0.1	terminating condition for pressure iterations (max cumulative density error $<$ 0.1%)
`omega`	0.5	relaxation parameter for Jacobi pressure iterations
`psi`	1.5	parameter of the implicit compressible pressure solver
Lennard-Jones potential that prevents pair instability		
`lj_cutoff`	0.6	cutoff distance
`lj_epsilon`	1.0×10^{-5}	depth of the potential well
`lj_sigma`	0.23	finite distance at which the potential is zero

Table S4. Simulation parameters for viscosity analysis simulation. Parameters beginning with a capital case letter are given in SI units, parameters beginning with a lower case letter are given in dimensionless units. Some of the technical parameters are skipped for brevity.

Parameter	Value	Short description
Length scale		
`Length_scale`	1.0×10^{-7}	kernel function cutoff h [m]
Outer fluid parameters		
`Fluid_density`	998.0	density of water [kg/m^3]
`Viscosity`	8.9×10^{-4}	dynamic viscosity of water [Pa s]
`Speed_of_sound`	1481.0	speed of sound [m/s]
`Temperature`	300.0	temperature [K]
`Kb`	$1.3806504 \times 10^{-23}$	Boltzmann constant [J/K]
Simulation parameters		
`skin`	0.12	skin thickness
`particle_diameter`	0.3	particle diameter
`timestep`	0.001	timestep size relative to the time scale
`max_rho_relative_error`	0.1	terminating condition for pressure iterations (max cumulative density error $<$ 0.1%)
`omega`	0.5	relaxation parameter for Jacobi pressure iterations
`psi`	1.5	parameter of the implicit compressible pressure solver
Lennard-Jones potential that prevents pair instability		
`lj_cutoff`	0.6	cutoff distance
`lj_epsilon`	1.0×10^{-5}	depth of the potential well
`lj_sigma`	0.23	finite distance at which the potential is zero
OBMD parameters		
`pxx`	1.0	background pressure
`pxy`	0.0	external xy shear stress
`pxz`	1.0	external xz shear stress
`buffer_relative_size`	0.2	buffer size relative to the simulation cell length
`shear_relative_size`	0.125	shear buffer size relative to the simulation cell length
`alpha`	0.7	scaling factor for desired number of particles in the buffer
`tau_usher`	30	relaxation time of the insertion algorithm

Table S5. Common simulation parameters for all acoustophoresis simulations. Parameters beginning with a capital case letter are given in SI units, parameters beginning with a lower case letter are given in dimensionless units. Some of the technical parameters are skipped for brevity.

Parameter	Value	Short description
Length and time scales		
`Length_scale`	1.0×10^{-7}	kernel function cutoff h [m]
`Time_scale`	1.0×10^{-8}	time scale [s]
Outer fluid parameters		
`Fluid_density`	998.0	density of water [kg/m^3]
`Speed_of_sound`	1481.0	speed of sound [m/s]
`Temperature`	300.0	temperature [K]
`Kb`	$1.3806504 \times 10^{-23}$	Boltzmann constant [J/K]
Simulation parameters		
`skin`	0.12	skin thickness
`particle_diameter`	0.3	particle diameter
`timestep`	0.003	timestep size relative to the time scale
`max_rho_relative_error`	0.1	terminating condition for pressure iterations (max cumulative density error $<$ 0.1%)
`omega`	0.5	relaxation parameter for Jacobi pressure iterations
`psi`	1.5	parameter of the implicit compressible pressure solver
Lennard-Jones potential that prevents pair instability		
`lj_cutoff`	0.6	cutoff distance
`lj_epsilon`	1.0×10^{-5}	depth of the potential well
`lj_sigma`	0.23	finite distance at which the potential is zero
DPD parameters (gas inside microbubble)		
`dpd_temperature`	0.001	DPD temperature
`dpd_cutoff`	0.6	DPD cutoff distance
`dpd_a_gas_gas`	2.0	conservative force parameter between gas particles
`dpd_gamma_gas_gas`	10.0	dissipative force parameter between gas particles
Lennard-Jones parameters for gas-shell interaction		
`lj_cutoff2`	0.6	cutoff distance
`lj_epsilon2`	0.01	depth of the potential well
`lj_sigma2`	0.3	finite distance at which the potential is zero
OBMD parameters		
`buffer_relative_size`	0.1	buffer size relative to the simulation cell length
`shear_relative_size`	0.125	shear buffer size relative to the simulation cell length
`alpha`	0.7	scaling factor for desired number of particles in the buffer
`tau_usher`	30	relaxation time of the insertion algorithm
Microbubble material		
`Shell_density`	1100.0	density of the shell material [kg/m^3]
`Shell_thickness`	15.0×10^{-9}	thickness of the shell [m]
`viscosity_shell`	0.1	small additional viscous force on shell particles
Microbubble elasticity		
`Yt`	2.64×10^{7}	Young's modulus
`nu`	0.5	Poisson ratio
`fscale`	0.0003	scaling factor in isotropic elastic model